Roles of the Atmospheric Heat Sources in Maintaining the Subtropical Convergence Zones: An Aqua-Planet GCM Study

YASU-MASA KODAMA

Department of Earth and Environmental Sciences, Hirosaki University, Hirosaki, Aomori, Japan

(Manuscript received 10 June 1997, in final form 4 February 1999)

ABSTRACT

The subtropical convergence zones (STCZs), that is, the Baiu frontal zone and subtropical portions of the South Pacific and South Atlantic convergence zones, are unique subtropical rainfall systems connected to the tropical monsoons to the west. An aqua-planet GCM without any land was used to study diabatic heating contributions in tropical monsoons and the STCZs that maintain the STCZs.

An STCZ was simulated in the GCM without any influence of land when a monsoonlike, namely, strong zonally localized off-equatorial heat source, was put in the Tropics. The monsoonlike heat source has two roles: 1) making a strong subtropical jet through a local Hadley circulation in the summer hemisphere and 2) making a low-level poleward moisture flow, which supplies considerable moisture to the STCZ. Upward motion maintained by the diabatic heating in the STCZ induces a low-level trough along the west and poleward side of the STCZ, keeping the vorticity balance between stretching and advection of low absolute vorticity air from the Tropics. This trough intensifies the low-level wind along the STCZ. This wind maintains strong convergence in the STCZ, together with the poleward moisture flow from the Tropics. The upward motion also induces an upper-level trough and ridge with the STCZ between, as a result of vorticity balance between shrinking and eastward vorticity advection by the mean westerlies. The radiation of a stationary Rossby wave from the STCZ was also suggested.

1. Introduction

The subtropics are characterized as dry zones in the global atmosphere. There are, however, three significant convergence zones that are intensified in summer, that is, the Baiu/Mei-yu frontal zone (BFZ) over East Asia and the western North Pacific, and the subtropical portions of the South Pacific convergence zone (SPCZ) over the South Pacific and of the South Atlantic convergence zone (SACZ) over the southern part of Brazil and the South Atlantic. In this study, they are referred to as subtropical convergence zones (STCZs) following Kodama (1993), and their locations are shown in Fig. 1 as long-term averaged outgoing longwave radiation (OLR) fields during the summer of each hemisphere.

The STCZs are unique rainfall systems in the global atmosphere, which are characterized by several intermediate features between tropical and midlatitudes rainfall systems. Active convection with considerable rainfall is one of their characteristics, which is similar to tropical systems. Monthly rainfall along the STCZs attains 300–500 mm during active periods of their intraseasonal variations (Kodama 1992), which is comparable to the ITCZ. The STCZs are also frontal zones like the outer boundary of a moist tropical or monsoonal air mass and are characterized by a weak or moderate temperature gradient and strong low-level humidity gradient. They are accompanied by an upper subtropical jet along the STCZ, and westerlies of the jet extend downward toward the earth's surface (Kodama 1992; Ninomiya 1984).

Important roles of the tropical monsoons for maintaining the STCZs have been suggested in many studies. For example, the STCZs commonly extend to the northeast [in the Northern Hemisphere (NH)] or the southeast [in the Southern Hemisphere (SH)] from active rainfall areas of the tropical monsoons, in spite of their variable topographical conditions. Both the BFZ and SACZ appear near the eastern coast of the continents, while the SPCZ is over the central portion of the South Pacific (Fig. 1). There is much observational evidence for coherent intraseasonal variations between the STCZs and adjacent tropical monsoons (e.g., Murakami 1984; Lau and Chan 1985; Chen and Chen 1993). Modeling studies also suggest the importance of the tropical monsoons to maintaining the STCZs. Gandu and Geisler (1991) and Figueroa et al. (1995) showed that strong diabatic heating over the Amazon Basin, not the Andes Corridor, is indispensable to forming the SACZ in their numerical

Corresponding author address: Dr. Yasu-Masa Kodama, Department of Earth and Environmental Sciences, Faculty of Science and Technology, Hirosaki University, Hirosaki, Aomori, 036-8561 Japan. E-mail: kodama@cc.hirosaki-u.ac.jp

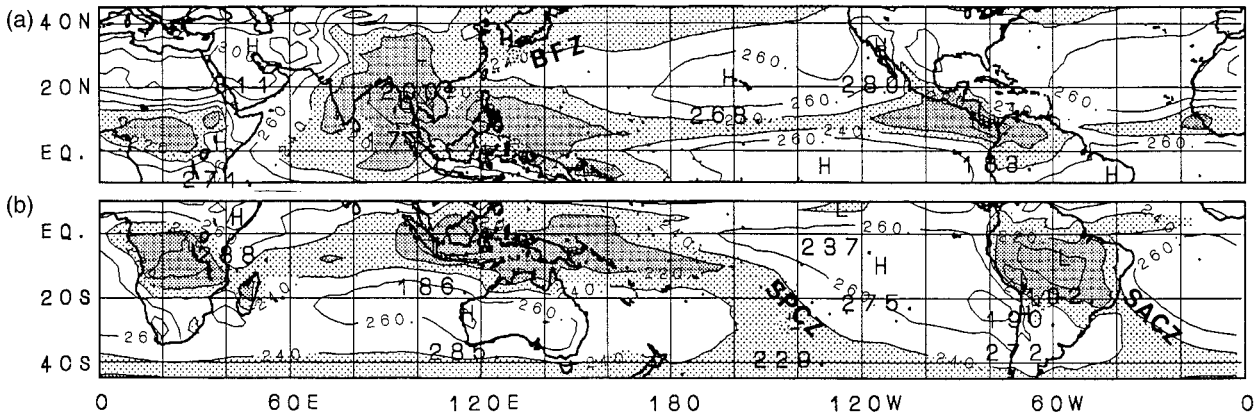

FIG. 1. (a) OLR distributions averaged for the NH summers (Jun–Aug) and (b) for the SH summers (Dec–Mar) between 1979 and 1986 after Kodama (1992) with minor modifications. Contour interval is 20 W m^{-2} and thick (thin) shading indicates OLR less than 220 W m^{-2} (240 W m^{-2}).

models. Kiladis et al. (1989) showed that the strength of the SPCZ in their general circulation model (GCM) was reduced when the tropical monsoon north of Australia disappeared. Recently, Ose (1998) showed in his GCM that deep convections in southeast Asia tend to form southwesterly low-level flow and upward motion southeast of Japan, which are considered to be the background of the BFZ.

First, this study will examine the roles of the tropical monsoons in forming the STCZs. In the real atmosphere and GCMs simulating the real atmosphere, the STCZs are affected by not only the monsoons but many other factors, including their surrounding topography and land–sea distribution. To exclude these geographical influences, we perform experiments using an aqua-planet GCM without any land, in which a monsoonlike, that is, strong and localized atmospheric heat source, is adopted. As shown later, a heat source away from the equator makes a rainfall zone in the subtropics similar to the STCZs. We study how the tropical heat source helps to maintain this rainfall zone.

Second, this study will examine the influence of the strong heating in the STCZs to atmospheric circulations. Observational studies (Vincent 1982; Yamazaki and Chen 1993) suggest unique local circulation around the STCZs when they are active, namely, a low-level trough elongated along the pole-westward side of the STCZs, and a coupled upper-level ridge and trough elongated along the west-poleward side and along the east-equatorward side of the STCZs, respectively. Yamazaki and Chen (1993), using a 2D quasigeostrophic model, suggested that strong heating in the BFZ can produce such circulation. Kalnay et al. (1986) also suggested that a trough of the SACZ was partly maintained by the heating in the SACZ in their GCM prediction experiment. In this study, we show that similar circulation appears around the rainfall zone in our aqua-planet GCM and discuss mechanisms of the circulation maintained by the diabatic heating based on a vorticity budget analysis. Moreover, we study the influence of the heating on global-scale circulations.

Several related studies were done on atmospheric responses to a localized heat source in the Tropics. Gill (1980) studied the response in a viscous linear model. A low-level depression forms around the heat source at the equator. As the heat source shifts to the north away from the equator, the depression is intensified and its center shifts to the northwest of the source. Using a simplified nonlinear model in which the mean upper westerlies in an NH winter are adopted, Hendon (1986) showed that the response in the upper-level atmosphere is strongly influenced by the nonlinear effect. When the heat source is strong, upper-level twin ridges in the subtropics induced by the source are not located to the west of the source as predicted in linear models; instead they are around the same longitude due to nonlinear effects. He also showed that the heat source radiates stationary Rossby wave trains into the midlatitudes. Ting and Held (1990) confirmed the importance of nonlinearity in the atmospheric response using an aqua-planet GCM. In their study, the center of the source was several degrees away from the equator and a rainfall zone extended toward the subtropics from the source [cf. Fig. 4c of Ting and Held (1990)]. Although this extension is similar to the STCZ shown in our study, they did not discuss it in detail.

Since much of the rainfall in the STCZs depends on the large-scale moisture circulation, not only simple models but full-physics GCMs (including the moisture-circulation process) are used to study the STCZs. Moreover, we need to study the atmospheric response to a tropical heat source away from the equator not by several degrees, as in Ting and Held (1990), but by 10° or more, like the monsoons in the real atmosphere, for example, around 10°S over the Amazon Basin and around 20°N over tropical Asia (Fig. 1). Our study is unique in studying the atmospheric response to a mon-

soonlike heat source, namely, a strong localized off-equatorial heat source, using an aqua-planet GCM.

In section 2, we describe our aqua-planet GCM and show the experimental design. In section 3, we show that formation of the STCZ in the GCM strongly depends on the latitude of the tropical heat source and discuss the roles of the source in forming the STCZ. In section 4, the relationship between rainfall activity in the STCZ and the surrounding atmospheric circulations are described. In section 5, we show that the STCZ in the GCM has several unique characteristics commonly observed in the STCZs in the real atmosphere. In section 6, we discuss the influence of the diabatic heating in the STCZ to local atmospheric circulations, based on a vorticity budget analysis. In section 7, we show a predominant circulation change induced by the cutoff of the heating in the STCZ. A stationary Rossby wave radiating from the STCZ is also suggested. In section 8, we summarize our results and show a possible scenario for the roles of the atmospheric heat sources in maintaining the STCZs.

2. Model description and experimental design

The aqua-planet GCM we utilize was developed by Numaguti (1993). A full description of the GCM is found in Numaguti (1993), and we briefly introduce it here. Resolution of the GCM is horizontally triangular-42 (corresponding to ~300 km) and vertically 16 sigma levels. Kuo (1974) is adopted as the convective parameterization scheme. Heat flux at the sea surface is evaluated by the bulk formulas depending on surface wind speed. To save computational time, the treatment of the radiative process is very simplified, especially by neglecting the absorption of shortwave radiation in the model atmosphere, that is, the atmosphere is heated only by the model ocean with a temporally fixed sea surface temperature (SST) through longwave radiation and sensible and latent heat fluxes. As is well known, most of the heat source of the real atmosphere is not the absorption of shortwave radiation, but outgoing energy from the earth's surface. Therefore, our treatment is an adequate approximation in spite of several departures in components of the energy balance from the real atmosphere.

The basic SST distribution adopted in the GCM is the same as in Numaguti (1993), in which the SST decreases with latitude from 300.5 K at the equator. Sea ice is removed for simplicity. To make a localized atmospheric heat source in the GCM, we put an oval-shaped warm water pool of 40° longitudinal width and 20° meridional extent on the base. The SST is 303 K over the pool, which is higher than the surrounding ocean by 2.5–6.0 K. As shown later, active convection is concentrated over the pool and acts as a strong localized atmospheric heat source. In the real atmosphere, tropical monsoons are induced by the land–ocean distribution. Nevertheless, the role of the monsoons as a heat source can be expressed by a mass of deep convection in our aqua-planet GCM.

We perform four experiments as follows. In experiment A, the warm water pool is centered at the equator to make an equatorial atmospheric heat source. In experiment B, to make an off-equatorial heat source, the whole SST field of experiment A is shifted northward by 10°, thus locating the center of the pool at 10°N. In experiment C, to make a heat source at the border of the Tropics, the SST field is the same as in experiment B except the pool is centered at 20°N. Experiment D is the same as experiment B except that the diabatic heating by the moist process is removed around the STCZ in the model to investigate the effect of heating in the STCZ on atmospheric circulation. Figure 2 shows the SST distributions adopted for each experiment. Although the coastlines are shown in many figures, they are included to show horizontal scales, but there is no land in the GCM.

Time integration is done for 200 days for each experiment, except in experiments B and D for which 400-day integrations are done to detect intraseasonal variations. We analyze the results after the 101st day, when the influence of initial conditions seems to be weakened sufficiently. Five-day averaged amounts are mainly analyzed in this study to remove short-period variations.

3. Appearance of the STCZ in the aqua-planet GCM and its dependency on the latitude of the tropical heat source

Since radiative processes in our GCM are very simplified, we need to check the performance of the GCM first. Figure 3 shows the zonally averaged latitude–height cross section of eastward wind speed and temperature in experiment A averaged for days 101–200. The GCM represents the basic structure of troposphere, namely, a tropopause, subtropical jets at ~30°N and ~30°S, and polar frontal jets at ~60°N and ~60°S. Similar results are obtained in the other experiments (not shown). In the Tropics, abnormal upper westerly winds, which may affect the Rossby wave propagation from the Tropics, appear. However, influence of the abnormal westerlies to the interaction between the tropical heat source and the subtropical rainfall, which we are studying, is not so strong, because upper-level easterlies dominate over the tropical heat source, as shown later in this section. To evaluate wave activity in the GCM, the standard deviations of day-to-day 500-hPa height variation are compared between the GCM and the real atmosphere using the National Centers for Environmental Prediction–National Center of Atmospheric Research (NCEP–NCAR) reanalysis data for 1988–95. The zonally averaged standard deviations in experiments A and B show meridional variations similar to long-term averaged variations observed in the real atmosphere during spring or fall and during the NH summer, respectively (not shown). Since the maxima of convective ac-

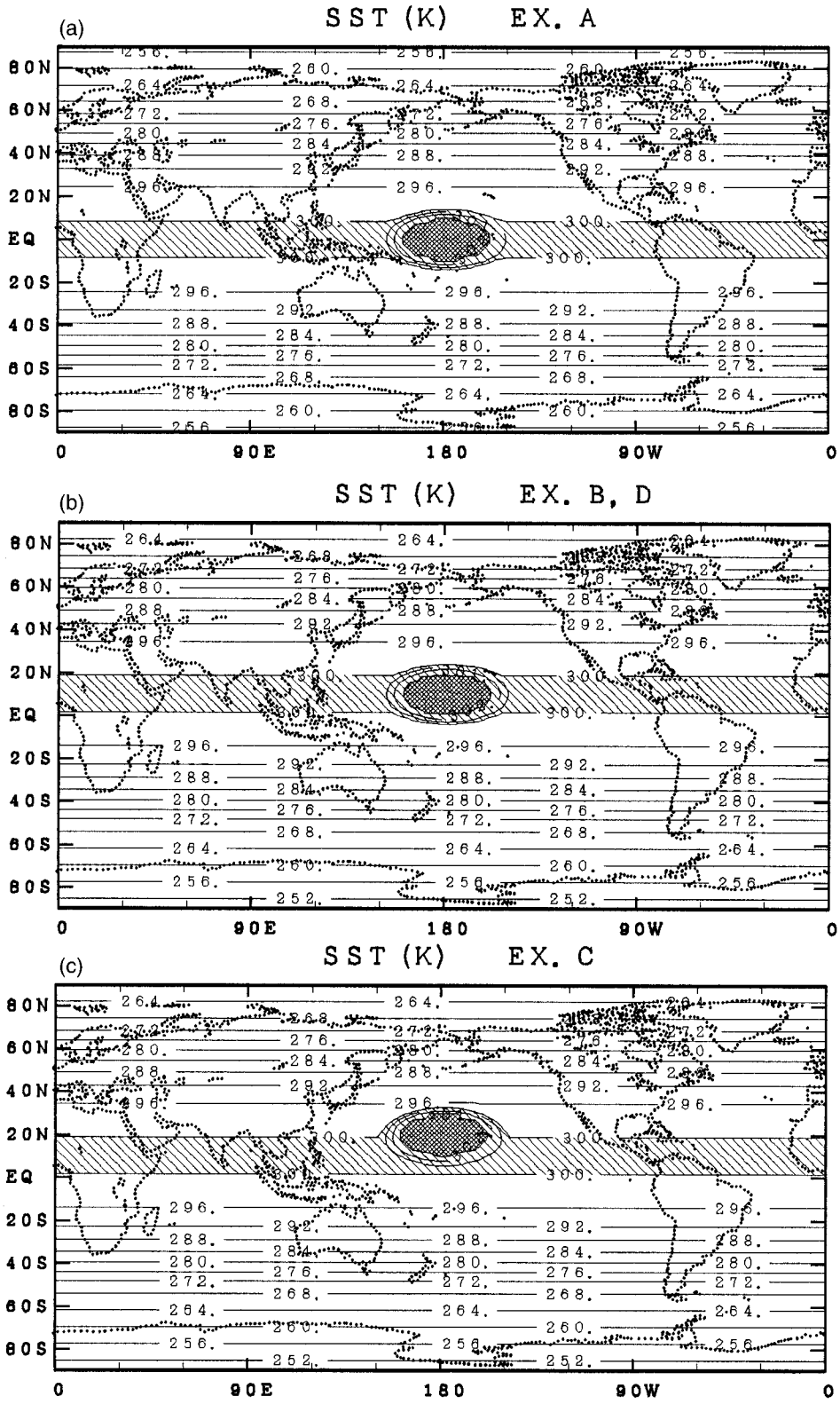

FIG. 2. SST distributions adopted for (a) experiments A, (b) B and D, and (c) C. Contour interval is 4 K below 300 K and 1 K above 300 K. Thick (thin) shading indicates SST higher than 303 K (300 K). Coastlines are shown only to indicate a horizontal scale, but the GCM includes no land.

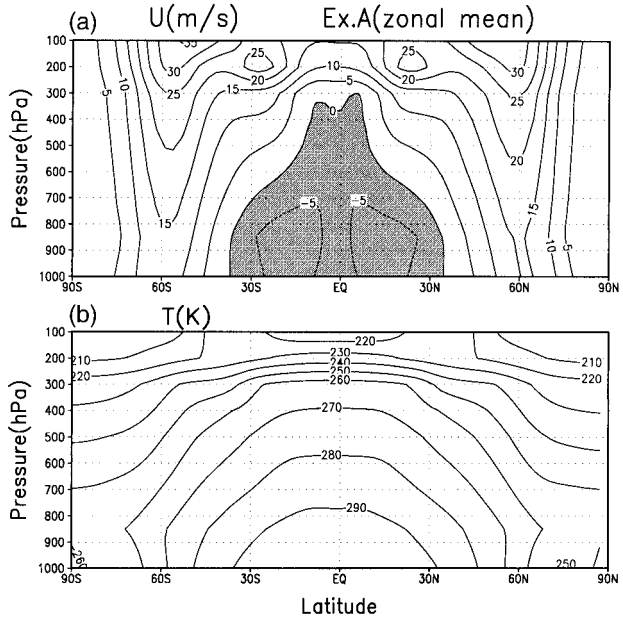

FIG. 3. Zonally averaged meridional cross sections of (a) westerly wind speed and (b) temperature in experiment A averaged for days 101–200. Shading in (a) indicates easterlies. Contour interval is (a) 5 m s^{-1} and (b) 10 K.

tivity in experiments A and B appear around the equator and 10°N as in spring or fall and in the NH summer in the real atmosphere, respectively, the GCM is considered to represent reasonable wave activity. These similarities between the GCM and the real atmosphere described above indicate that the performance of the GCM is adequate for studying the dynamics of the STCZs.

The upper panels of Fig. 4 show rainfall distributions around the warm water pool in experiments A, B, and C averaged for days 101–200. In every experiment, rainfall is active over the pool, although strong rainfall is concentrated over the southern portion of the pool in experiment C. Rainfall intensity over the pool is ~10 mm day^{-1}, which is comparable to the intensity observed in the tropical monsoons (cf. Jaeger 1976; Janowiak et al. 1995). This guarantees that the strong rainfall over the pool acts as an atmospheric heat source comparable to the tropical monsoons in the real atmosphere.

Rainfall activity in the subtropics is variable among the experiments. In experiment A, rainfall in the subtropics is scarce, although weak rainfall appears to the northeast and southeast of the tropical heat source. In experiment B, a significant rainfall zone extends northeastward from the source. In experiment C, a rainfall zone also extends from the source, although its direction is more zonal than that in experiment B. Hereafter, we refer to the significant rainfall zone in the subtropics observed in experiments B and C as the model STCZ, and the STCZs in the real atmosphere as the real STCZs. In section 5, we show that the model STCZ has several large-scale features observed in the real STCZs.

To clarify why the subtropical rainfall is different among the experiments, large-scale circulations are examined. The middle and bottom panels of Fig. 4 show the fields of 200-hPa height and sea level pressure (SLP), respectively. In experiment A, twin anticyclones appear in the upper troposphere at almost the same longitude as the heat source and twin troughs of subtropical jets downstream. These features are similar to the results of nonlinear modeling studies by Hendon (1986) and by Ting and Held (1990). In experiments B and C, the upper anticyclone is intensified in the NH and extends eastward along the southeastern edge of the model STCZ. The spatial relationship between the rainfall of the model STCZ and surrounding height field is similar to the observed one for the real STCZs (Vincent 1982; Yamazaki and Chen 1993). We show that the unique height field around the model STCZ becomes significant when the STCZ's rainfall is strong in section 4 and that the height field is maintained by the diabatic heating in the model STCZ in section 6.

In the lower troposphere, a localized depression forms around the tropical heat source in every experiment. In experiments B and C, the depression is intensified and strongly penetrates a high belt in the NH subtropics. Therefore, the eastward pressure gradient along the eastern edge of the depression is much stronger in these experiments than in experiment A (Fig. 4). A strong poleward flow may appear in the strong pressure gradient in experiments B and C and transport much moisture toward the subtropics. Actually, a vertically integrated poleward moisture flux across 20°N toward the subtropics is much larger in experiments B and C than in experiment A (Fig. 5). Dependency of the STCZ's formation on the latitudes of the heat source can be mainly ascribed to the poleward moisture transport, which is intensified as the source shifts away from the equator. This is because the transport is a major moisture source for active rainfall in the STCZ, as will be shown in section 4. Similar poleward moisture transport has been noted as a major moisture source of the real STCZs (Matsumoto et al. 1971; Kato 1989; Kodama 1993).

Figure 6a shows the *u* component of the 200-hPa-level winds in experiment B that were averaged for days 101–200. As stated previously, local easterlies appear around the tropical heat source within the abnormal westerlies developed in the Tropics. Since the easterlies extend to 15°–20°N, nearly as much as the latitudes of poleward extension of the upper easterlies near the real STCZs,[1] we can expect that interaction between the Tropics and subtropics through Rossby wave propaga-

[1] According to the composite height fields at the 300-Pa level shown in Kodama (1992), the latitude changing from the easterlies to the westerlies is ~25°N around the BFZ, and ~15°S around the SPCZ and the SACZ.

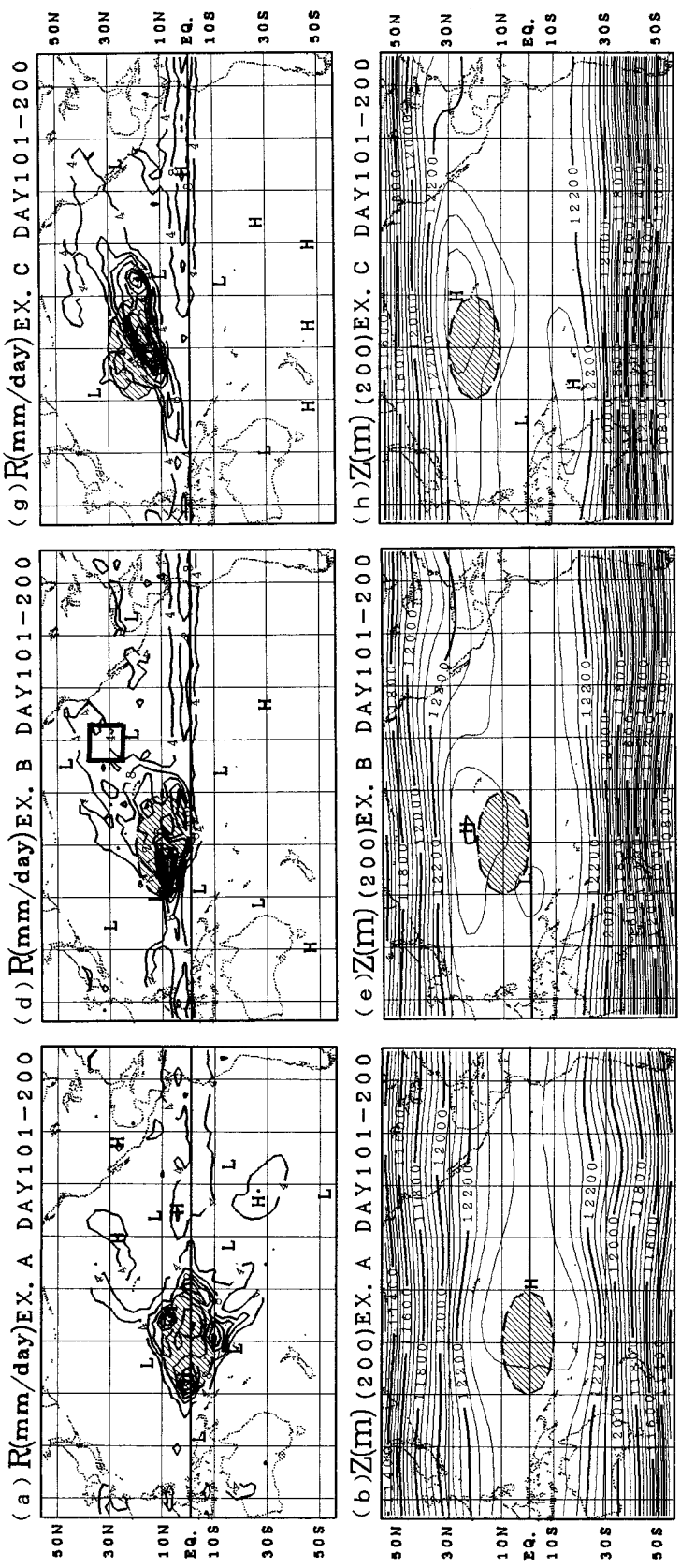

FIG. 4. Distributions of (upper panels) rainfall intensity, (middle panels) 200-hPa height, and (bottom panels) SLP averaged for days 101–200. Left, middle, and right columns are the results for experiments A, B, and C, respectively. The hatched oval in each panel indicates the location of the warm water pool for each experiment. Contour intervals are 4 mm day^{-1}, 50 m, and 4 hPa for the upper, middle, and bottom panels, respectively. The rectangular region shown in (d) is the area used to evaluate the rainfall intensity of the STCZ.

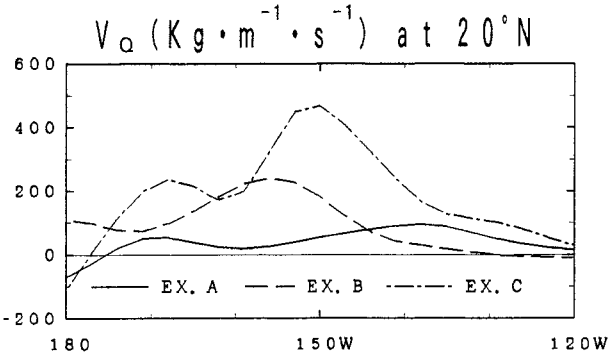

FIG. 5. Vertically integrated poleward moisture flux across 20°N between 120°W and 180° in experiments A (solid line), B (dashed line), and C (dash–dot line) averaged for days 101–200.

tion is not unrealistic around the tropical heat source in the GCM.

As shown in Fig. 6a, the modeled subtropical jet in the NH is nearly as weak as in the climatology of the summer hemisphere in the real atmosphere. However, a streak of strong subtropical jet appears around ~30° north of the heat source. This streak, together with a corresponding streak in the SH, is maintained by the acceleration due to upper-level divergent outflow to the subtropics from the heat source (Fig. 6b). This means that a local Hadley circulation maintains the streaks. Similar subtropical jet streaks intensified by the tropical monsoons in the summer hemisphere are observed in the real atmosphere (Hurrell and Vincent 1990, 1991).

Generally, westerlies of subtropical jets are significant in the upper troposphere and disappear in the lower troposphere (Palmen and Newton 1969), except over the areas of strong low-level baroclinicity, such as the wintertime in East Asia, where the westerlies sometimes extend to the lower troposphere. On the other hand, westerlies of the subtropical jets extend to the surface in both the model and real STCZs when they are active (Fig. 12c of this study; Kodama 1992), though a low-level temperature gradient across the STCZs is not strong (e.g., Ninomiya 1984; Kodama 1992). Without these winds along the real and model STCZs in the lower troposphere, the poleward moisture flow maintained by the tropical heat source might pass under the subtropical jet to the midlatitudes and provide no rainfall in the subtropics. In fact, a significant low-level wind along the STCZs appears and strong moisture–flux convergence with poleward flow is maintained in the STCZs. We show in section 4 that the low-level wind along the STCZ appears in the active periods of the STCZ and that the low-level wind is maintained by strong diabatic heating in the STCZ in section 6.

The BFZ extends nearly zonally, while the SPCZ and SACZ extend diagonally in the real atmosphere (Fig. 1). The tropical monsoons accompanied by the BFZ are located at 10°–20°N, while those by the SPCZ and SACZ are at 5°–10°S (Fig. 1). The relationship between

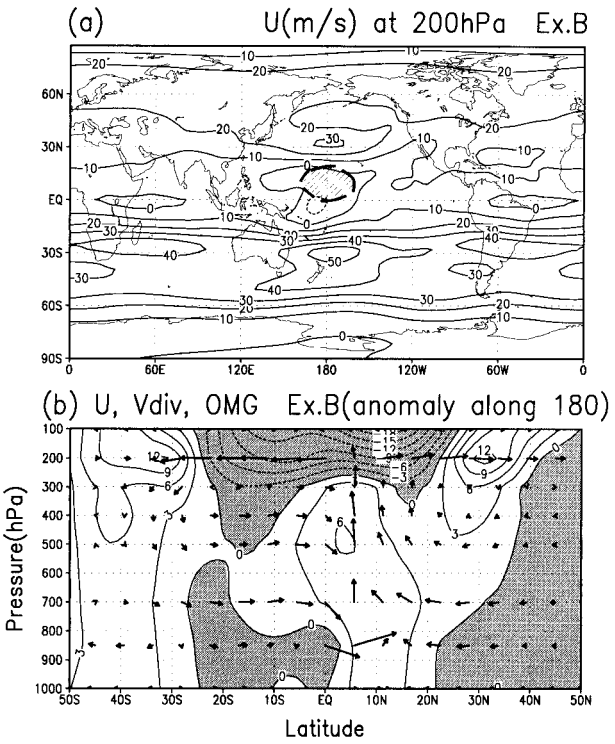

FIG. 6. (a) Mean field of westerly wind speed at the 200-hPa level in experiment B averaged for days 101–200, and (b) the meridional cross section of anomaly of westerly wind (contours) and north–south component of divergent wind and omega (vectors) along 180° from the zonal mean. Contour intervals are (a) 10 m s^{-1} and (b) 3 m s^{-1}. Increments of 10° lat and 100-hPa pressure correspond to 5 m s^{-1} and 2×10^{-3} hPa s^{-1}, respectively, in (b). The hatched oval in (a) indicates the area of the warm water pool.

the direction of the model STCZ and the latitude of the tropical heat source observed in experiments B and C suggests that a higher-latitude topical heat source makes the STCZ more zonal. This may be a reason why the BFZ extends more zonally than the other real STCZs.

4. Circulation change accompanied by rainfall activity of the model STCZ

Rainfall activity of the real STCZs shows significant intraseasonal variations (e.g., Huang and Vincent 1983; Murakami et al. 1986; Chen et al. 1988; Kodama 1993). Figure 7 shows temporal variation of rainfall intensity of the model STCZ in experiment B during days 101–400 over the reference area shown in Fig. 4d. Short-period variations are already removed because we use the 5-day averaged data. Variations of an intraseasonal timescale are significant in the rainfall activity of the model STCZ.

Circulation changes that accompany the intraseasonal variations may provide useful information about the relationship between rainfall activity of the STCZ and the surrounding circulations. To study the changes, we define active and break periods of the STCZ as the periods

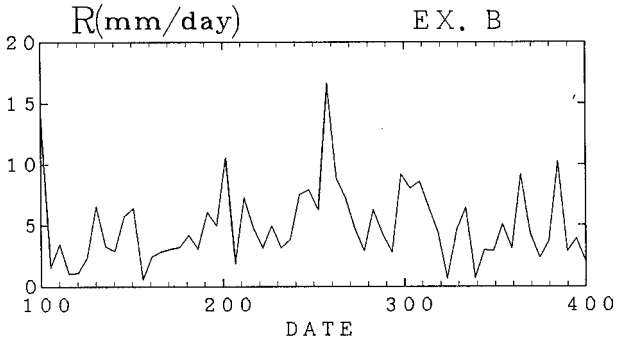

FIG. 7. Temporal variation of the rainfall intensity of the model STCZ (averaged over the rectangular area shown in Fig. 4d) in experiment B during days 101–400.

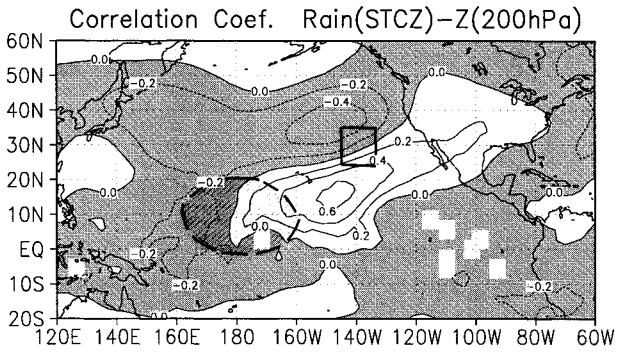

FIG. 9. Correlation coefficient between westerly wind at the 200-hPa level and rainfall intensity of the model STCZ over the rectangular area shown in the panel in experiment B. Contour interval is 0.2. The hatched oval indicates the area of the warm water pool.

when the 5-day averaged rainfall intensity of the STCZ, shown in Fig. 7, is more than 7 mm day^{-1} and less than 3 mm day^{-1}, respectively. Thirteen active and 18 break periods are selected from the total of sixty 5-day periods during days 101–400.

Figure 8 shows eastward and poleward moisture transports across 160°W and across 20°N, respectively, averaged for the active and break periods. The poleward transport toward the STCZ, maintained by the tropical heat source as shown in section 3, increases in the active periods around 140°W south of the reference area (Fig. 8b). This indicates the important roles of the poleward moisture transport in forming the STCZ. Another significant change appears in the eastward transport along the STCZ (Fig. 8a). This is ascribed to appearance (disappearance) of the low-level southwest (east and poleward) wind along the STCZ in the active (break) periods. In the active periods, two intensified moisture transports shown in Fig. 8 meet in the STCZ and maintain the strong rainfall in the STCZ. In the break periods, such moisture flux convergence is not expected because the low-level southwest wind along the STCZ has disappeared.

Figure 9 shows the correlation coefficient between rainfall intensity of the model STCZ over the reference area shown and the 200-hPa height. A dipole pattern, that is, a negative correlation around 35°N and 150°W and a positive correlation around 15°N and 150°W, indicates the development of a trough and ridge around the STCZ when the STCZ is active. This pattern is significant since the absolute amount of the correlation coefficient at the dipole is 0.4–0.6 and exceeds the 95% significant level: 0.27 for the sixty 5-day samples. Similar relationships between rainfall activity of the real STCZ and development of the subtropical jet trough have been observed in the work of Huang and Vincent (1983), Kalnay et al. (1986), and Kiladis and Weickmann (1992).

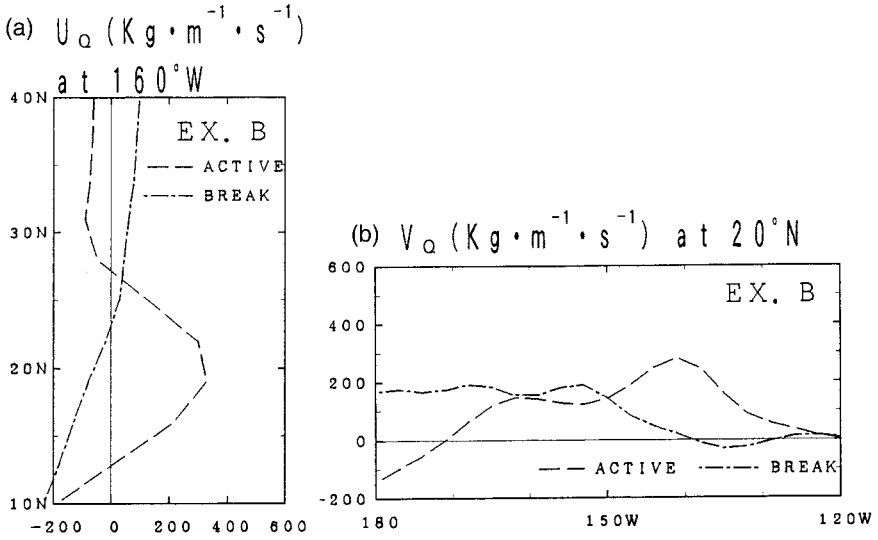

FIG. 8. (a) As in Fig. 5 except for the eastward moisture flux across 160°W for the active (dashed line) and break (dash–dot line) periods of the model STCZ in experiment B. (b) As in (a) except for the poleward moisture flux across 20°N.

Development of the low-level southwest wind along the model STCZ and upper-level trough of the subtropical jet is in phase with the rainfall activity of the STCZ. We discuss mechanisms of this connection using a vorticity budget analysis in section 6.

5. Large-scale characteristics of the model STCZ in its active periods

We show that the model STCZ in the active periods has several unique characteristics of the real STCZs. The outstanding characteristics of the real STCZs can be summarized as follows (Kodama 1992; Ninomiya 1984; Vincent 1982; Yamazaki and Chen 1993): 1) much rainfall activated by strong moisture–flux convergence; 2) active convection maintained by strong convective instability generated by large-scale differential advection, especially by the poleward moisture flow from the Tropics; 3) weak or moderate temperature gradient and strong moisture gradient in the lower troposphere bounding the moist monsoon or tropical air mass; and 4) a low-level trough elongated along the west and poleward side of the STCZs, and upper-level trough and ridge patterns appearing west and east of the STCZs, respectively.

Figure 10 shows composite fields of rainfall intensity, 200-hPa height, and SLP during the active periods for the model STCZ in experiment B (left column) and for the BFZ after Kodama (1992) for comparison (right column). We show the fields for the BFZ only as examples; similar characteristics are commonly observed among the real STCZs (Kodama 1992). Figures 10d and 10f show the amount of high clouds with tops higher than the 400-hPa level, as an indicator of rainfall activity, and 1000-hPa height instead of SLP, respectively. Figure 10e showing 200-hPa height is not from Kodama (1992) but was prepared for this study using the same method and objective analysis data as in Kodama (1992).

In both the model STCZ and BFZ, rainfall and high cloudiness are concentrated along a narrow zone. Rainfall intensity in the model STCZ is more than 10 mm day^{-1}, which is as much as in the real STCZs in their active periods (Kodama 1992). In the upper troposphere, a strong subtropical jet flows in subtropical latitudes ($\sim$35°N) and both STCZs extend along the jet ahead of a trough. Moreover, a narrow upper-level ridge extends parallel to the STCZs at $\sim$1000 km to the southeast. In the lower troposphere, a narrow trough extends along the northwestern side of the STCZs.

Figure 11 shows composite fields of vertically integrated moisture flux and its convergence (upper panels), generation of convective instability by the differential advection process between 925- and 450-hPa levels (middle panels), and specific humidity at the 850-hPa level (bottom panels) during the active periods for the model STCZ (left column) and for the BFZ (right column).

Both the model STCZ and BFZ are characterized as convergence zones between the moist poleward flow from the Tropics and the southwest or west-southwest flow along the STCZs. Convergence of the moisture flux is $\sim$10 mm day^{-1} along both, nearly as much as the rainfall intensity there. Destabilization is strong along both STCZs with the amount of ~ -1 K day^{-1} (100 hPa)$^{-1}$. Moreover, the model STCZ north of 30°N is accompanied by a low-level humidity gradient as strong as in the BFZ. South of 30°N, the gradient is obscure in the model STCZ due to a strong dry area around 20°N and 145°W. Strong subsidence maintains this dry area, but its existence in the real atmosphere is uncertain. Low-level temperature gradient across the model STCZ and the BFZ is not strong (0–5 K (1000 km)$^{-1}$ at 850 hPa) (not shown).

The model STCZ in its active periods has all of the outstanding characteristics of the real STCZs. This means that a monsoonlike, namely, strong localized off-equatorial heat source in the Tropics, can form an STCZ without any influence of topography and land–sea distribution.

6. Influence of the diabatic heating of the STCZ

As shown in section 4, unique height fields appear around the STCZ when the rainfall of the STCZ is intensified. In this section, we show that these fields are maintained by strong diabatic heating in the STCZ.

First, general atmospheric responses to a heat source in the subtropics are discussed based on a vorticity budget analysis after Sardeshmukh and Hoskins (1985). When we neglect the vertical advection and twisting terms, which are relatively small, the vorticity equation in equilibrium may be approximated as,

$$\mathbf{v} \cdot \nabla(f + \zeta) = -(f + \zeta)\nabla \cdot \mathbf{v} - \epsilon\zeta,$$

where $\mathbf{v} = (u, v)$, f, ζ, and ϵ are horizontal velocity, Coriolis parameter, relative vorticity, and the coefficient of Rayleigh friction, respectively.

In the subtropics where f is much larger than in the Tropics, low-level convergence and upper-level divergence induced by the upward motion maintained by the atmospheric heating form a strong vorticity source and sink, respectively. When the strength of the vorticity source and sink exceeds the viscous vorticity dissipation, the source and sink should be canceled by advection of absolute vorticity. In the lower troposphere, where mean westerlies are weak, this balance may approach the Sverdrup balance,

$$\beta v = -f\nabla \cdot \mathbf{v},$$

where $\beta = \partial f/\partial y$. A poleward wind, which advects relatively low, absolute vorticity air, is required in the heating area. This means that a depression forms west of the heat source. In the upper troposphere, where a mean westerly is strong, the vorticity balance may approach the following:

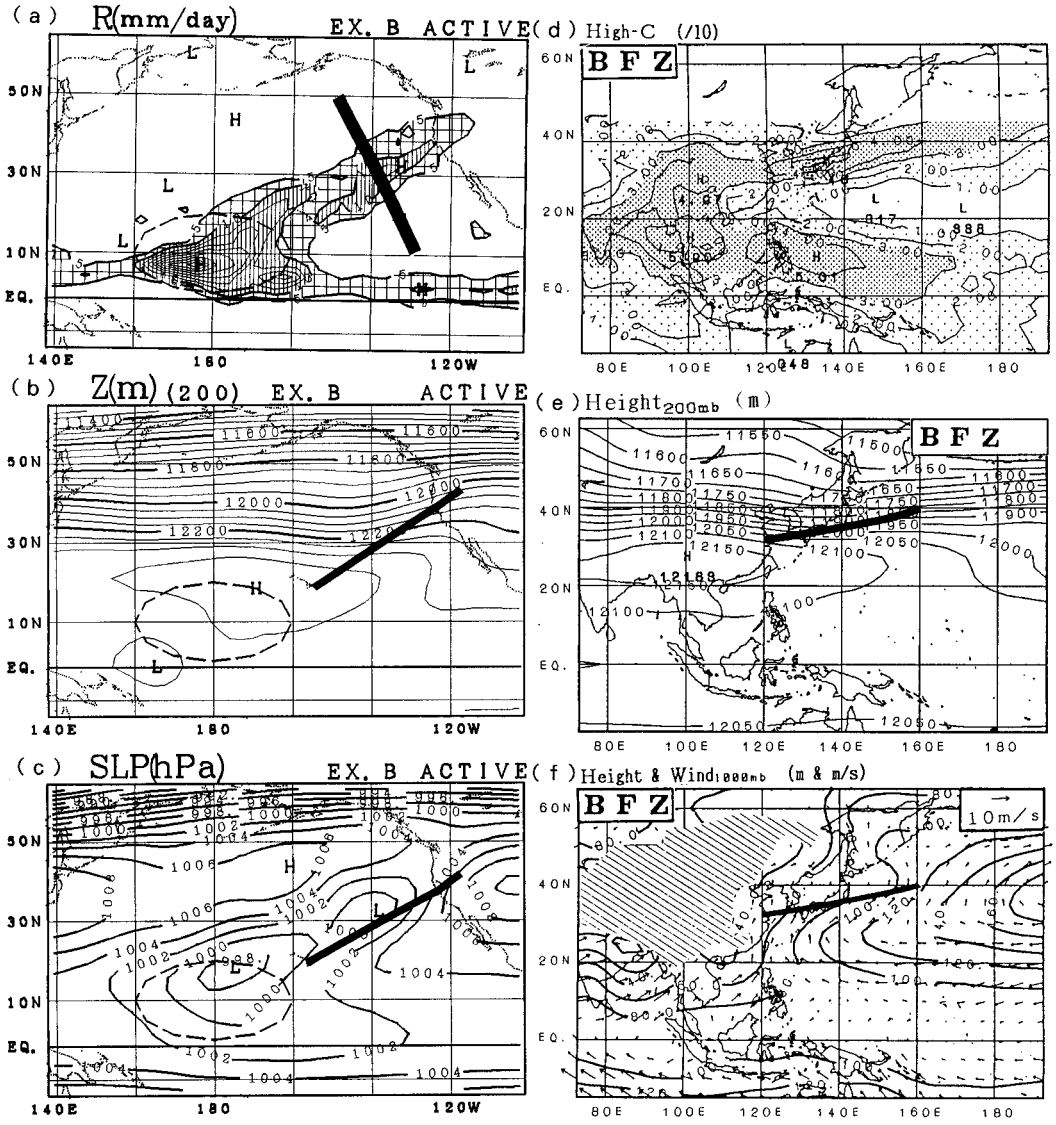

FIG. 10. Left column shows composite fields around the model STCZ in its active periods: (a) rainfall intensity, (b) the 200-hPa height, and (c) SLP. Right column is the same as the left column except around the Baiu frontal zone for its active periods [after Kodama (1993)]: (d) amount of high clouds with tops above the 400-hPa level, (e) the 200-hPa height, and (f) wind and height at 1000 hPa. Contour intervals are 5 mm day^{-1} in (a), 50 m in (b) and (e), 2 hPa in (c), 0.1 in (d), and 20 m in (f). Ovals enclosed by the dashed line shown in the left column indicate the areas of the warm water pool. (d) and (f). The thick solid line in (a) indicates the position of the cross sections shown in Fig. 14.

$$u\frac{\partial \zeta}{\partial x} = -(f + \zeta)\nabla \cdot \mathbf{v},$$

that is, the vorticity sink is canceled by positive vorticity advection from the west. This means that trough and ridge patterns form west and east of the heat source, respectively, to maintain a westward vorticity gradient around the heating area.

Since the model STCZ is quasi-stationary in its active periods (not shown), equilibrium is a proper approximation. We then confirm these balances for the model STCZ. Figure 12a shows height and wind divergence at 850 hPa in the active periods of experiment B. As stated previously, a trough forms on the northwestern side of a convergence zone corresponding to the STCZ, and a strong southwest wind appears along the STCZ. As shown in Fig. 12b, a strong southwest wind advects relatively low absolute vorticity air from the lower latitudes. The balance between the advection of absolute vorticity and generation of vorticity by stretching is rather good (Figs. 12c and 12d). Since there should be no trough on the STCZ, but one on the northwestern side of the STCZ to maintain the strong southwest wind along the STCZ, the northwestward shift of the trough

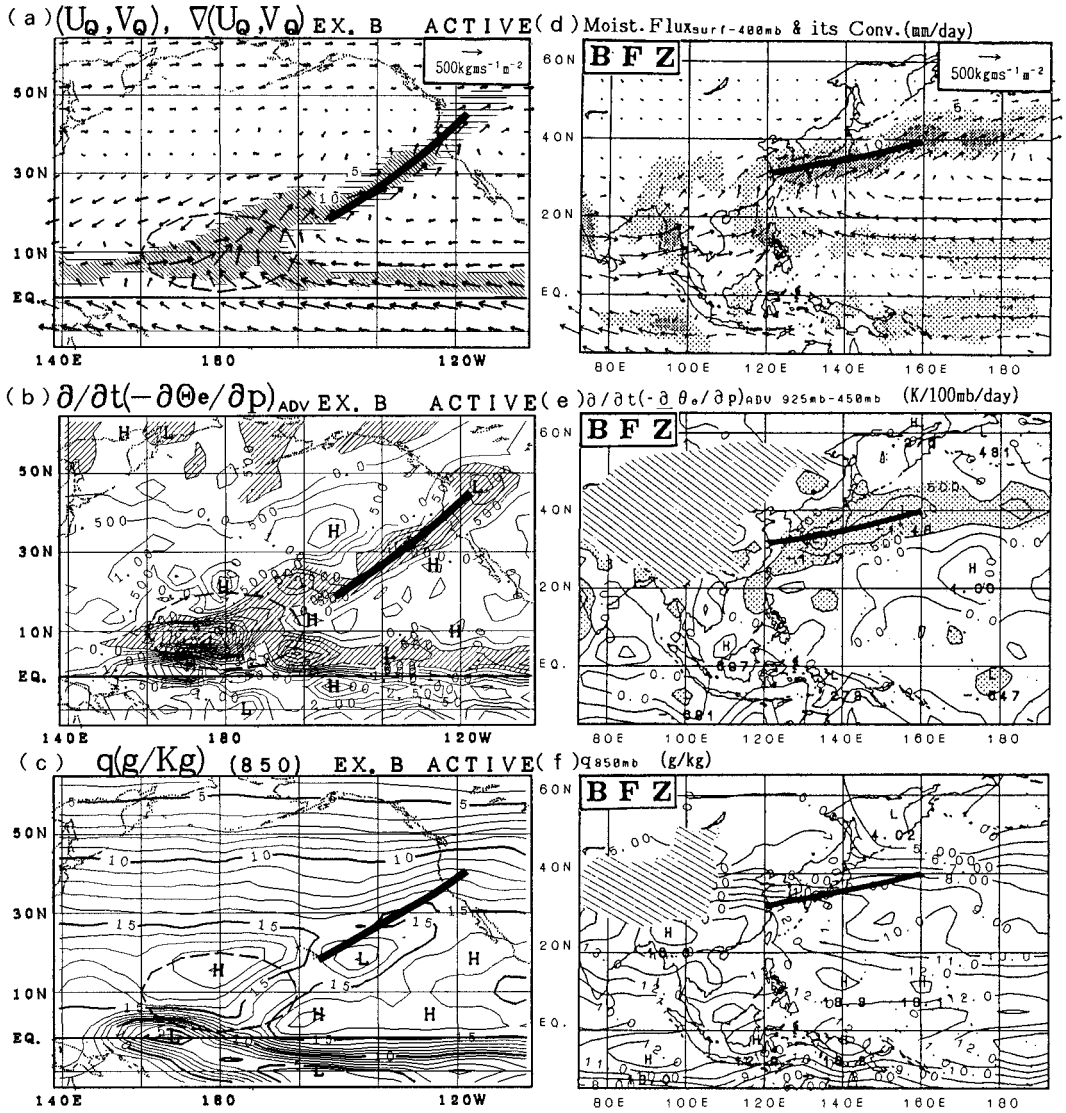

FIG. 11. (a) Composite fields of (top panels) vertically integrated moisture flux between the surface and the 400-hPa level and its convergence, (middle panels) generation of the convective instability evaluated between the 925-hPa and 450-hPa levels, and (bottom panels) specific humidity at the 850-hPa level. Left and right columns are for the model STCZ in experiment B and the BFZ (after Kodama 1992), respectively, in their active periods. Moisture flux convergence more than 5 mm day^{-1} (10 mm day^{-1}) is thin (thick) shaded in (a) and (d). Contour interval is 0.5 K day^{-1} (100 hPa)$^{-1}$ in (b) and (e), and 1.0 g kg^{-1} in (c) and (f). Oval enclosed by a dashed line in each left panel indicates the area of the warm water pool. Positions of the model STCZ and the BFZ are shown by thick solid lines.

is ascribed to upward motion induced by the diabatic heating in the STCZ.

In the upper troposphere, a trough (ridge) appears to the northwest (southeast) of the divergent axis (Fig. 13a). This coupled trough and ridge maintains a strong eastward gradient of absolute vorticity around the STCZ (Fig. 13b). A west-southwest wind along the subtropical jet advects relatively larger absolute vorticity from the trough to the STCZ, where vorticity advection balances the vorticity sink by divergence accompanied by strong upward motion along the STCZ. This means that the coupled trough and ridge are maintained by the diabatic heating along the STCZ.

The vertical connections of these trough and ridge patterns are displayed in a cross section of the STCZ (Fig. 14a). To describe the height change accompanied by the heating in the STCZ, the figure shows anomaly height, defined as the height difference between the active periods and the whole period (days 101–400). Rainfall intensity across the STCZ is shown in Fig. 14e. Consistent with the previous discussions, a low-level trough and upper-level coupled trough–ridge exist along

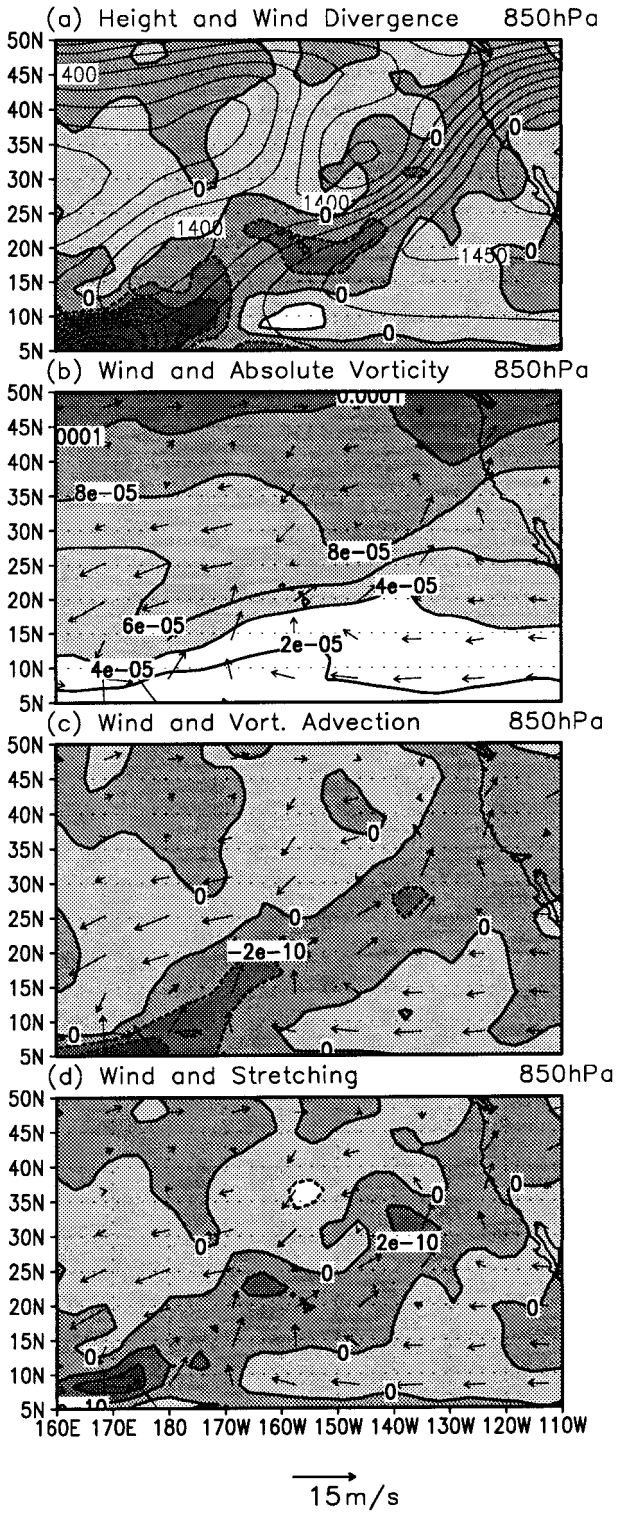

FIG. 12. Composite fields of the model STCZ in the active periods of experiment B at the 850-hPa level: (a) height (thin contours at 10-m interval) and horizontal wind divergence (thick contours at 3×10^{-6} s^{-1} interval), (b) wind (vectors) and absolute vorticity (contours at 2×10^{-5} s^{-1} interval), (c) wind and vorticity tendency by horizontal advection, and (d) wind and vorticity tendency by stretching. Contour intervals are 2×10^{-10} s^{-2} in (c) and (d).

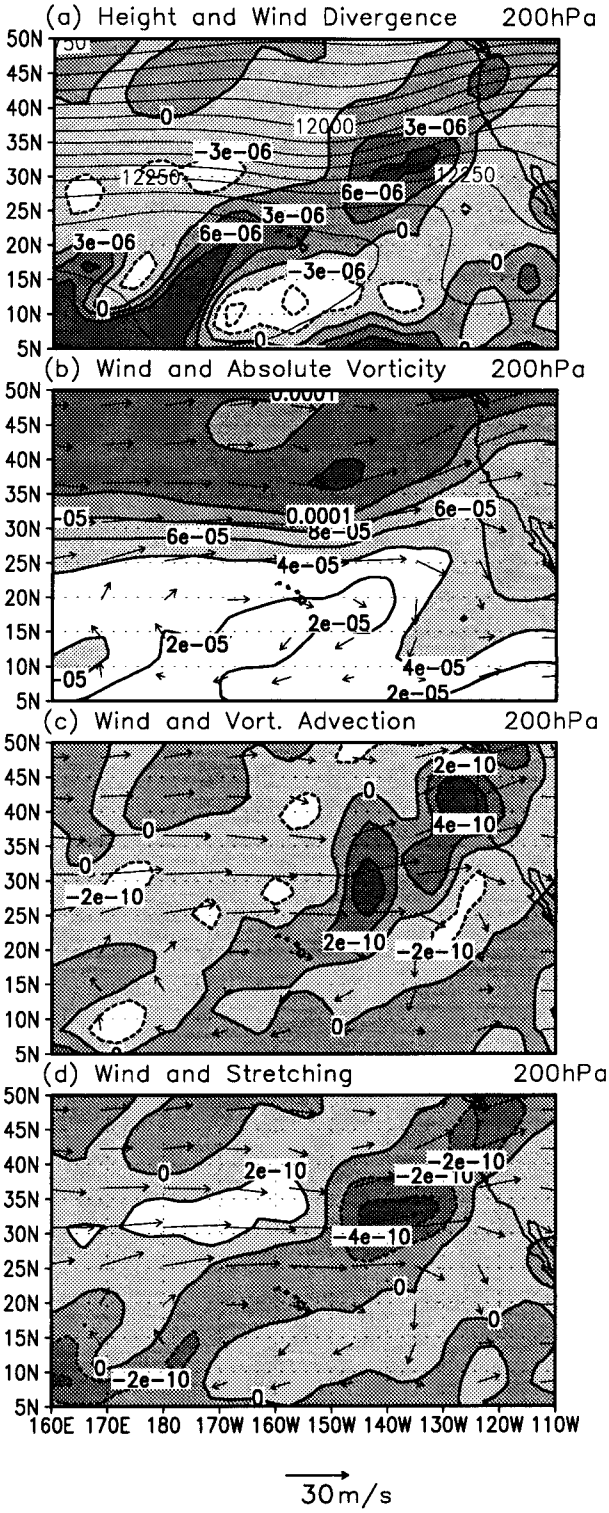

FIG. 13. As in Fig. 12 except at the 200-hPa level.

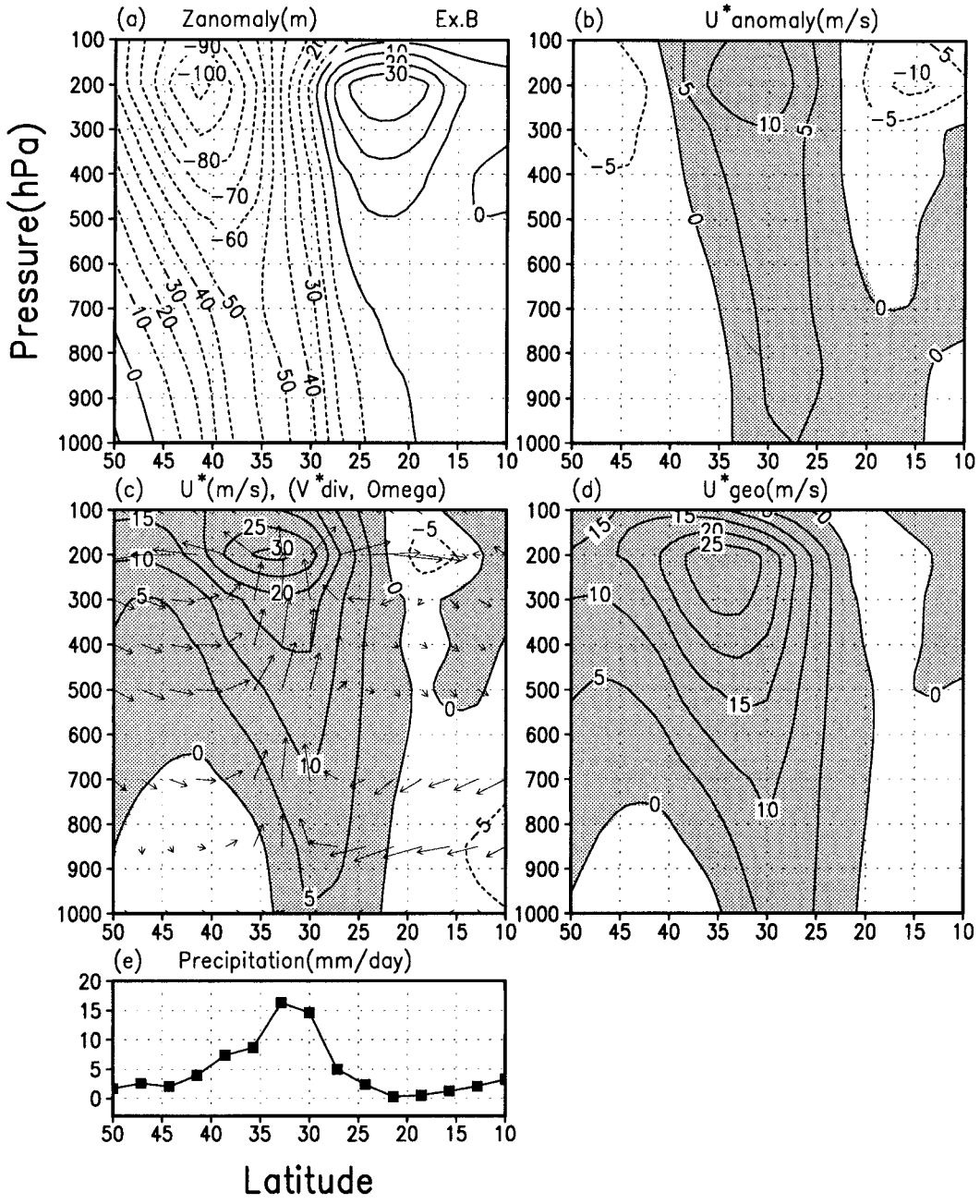

FIG. 14. Composite cross sections of the model STCZ for the active periods of experiment B: (a) height anomaly from the mean height averaged for the entire period of experiment B, (b) as in (a) except for the component of wind anomaly parallel to the STCZ, (c) wind component parallel to the STCZ and secondary circulation of the STCZ (component of the divergent wind normal to the STCZ and omega), (d) component of the geostrophic wind parallel to the STCZ, and (e) rainfall intensity. Contour interval is 10 m in (a). Contour interval is 5 m s^{-1} and shading indicates more than 0 m s^{-1} in (b), (c), and (d). Increments of 10° lat and 100-hPa pressure correspond to 4 m s^{-1} and 2×10^{-3} hPa s^{-1}, respectively, in (c).

the sides of the rainfall zone (cf. Fig. 14e). These troughs and ridge are connected through a poleward inclined trough–ridge system, as pointed out by Vincent (1982) for the SPCZ, and Yamazaki and Chen (1993) for the BFZ. Actually, Fig. 14a is similar to the observed anomaly height for the BFZ in its active periods, as shown in Fig. 14 of Yamazaki and Chen (1993).

The unique height field is related to the wind field around the STCZ. As shown in Fig. 14b, the wind component along the STCZ is intensified throughout the

troposphere in the active periods, accompanied by the intensified height gradient in the STCZ (cf. Fig. 14a). In the active periods, the strong wind of the subtropical jet extends downward to the surface (cf. Fig. 14c), although the wind direction veers somewhat with altitude from west-southwest at the 200-hPa level to southwest at the surface. The wind along the STCZ is as much as the anomaly wind in the lower troposphere (cf. Fig. 14b); namely, the low-level southwest wind appears in the active periods of the STCZ, as stated previously. The low-level southwest wind is related to the height field geostrophically because the wind component along the STCZ almost agrees with those of geostrophic wind (cf. Figs. 14c and 14d).

7. Effect of switching off the heating in the STCZ

We now show the results of experiment D, which is the same as experiment B except diabatic heating in the model STCZ is switched off. In this experiment, humidity in the atmosphere is removed and air temperature is replaced by virtual temperature to maintain the hydrostatic balance at every time step over the region between 5°–30°N and 115°–160°W. This dry region includes the original position of the model STCZ in experiment B, but extends the region eastward and equatorward. Since the artificial cutoff of rainfall affects large-scale circulation, unnaturally strong rainfall appears near the eastern and southern boundaries of the dry region. Since it may affect circulation to be studied around the original position of the STCZ, we extend the region to keep the unnatural rainfall at the border away from the original position.

To compare the composite charts for the active periods of experiment B, we make composite charts for experiment D for the periods when a trough of the subtropical jet was intensified. This is because rainfall in the STCZ is already removed in experiment D, and the trough was also intensified in the active periods of experiment B.[2] We selected the periods when a trough of subtropical jet is intensified northeast of the tropical heat source; namely, 200-hPa wind speed over the reference area shown in Fig. 15b is stronger than 12 m s^{-1}. The periods are referred to as active periods of experiment D. There are 17 active periods in experiment D out of a total of sixty 5-day periods.

The large-scale circulation changes drastically in experiment D. A subtropical-jet trough northeast of the tropical heat source penetrates to lower latitudes in experiment D than in experiment B (Figs. 10b and 15b). This deep trough is also found in the mean field averaged over all periods of experiment D (not shown). This trough should be induced by the tropical heat source.

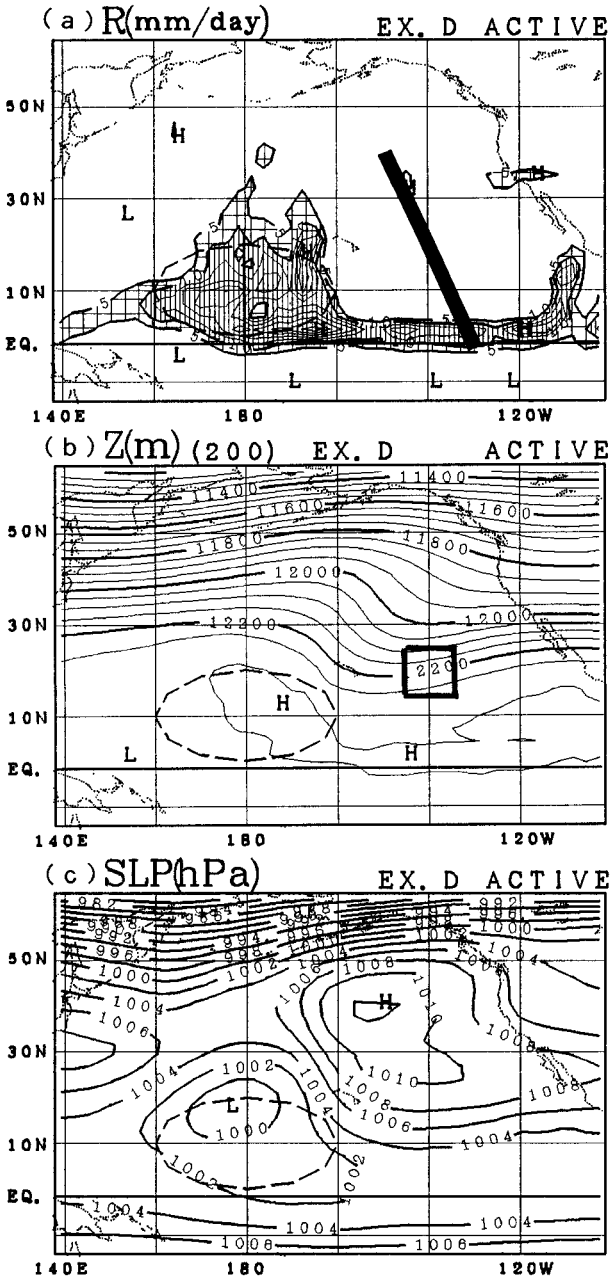

FIG. 15. As in the left column of Fig. 10 except for experiment D. The thick solid line in (a) shows the position of the cross sections in Fig. 16. The rectangular region in (b) is the area used to evaluate the wind speed of the subtropical jet.

The upper-level ridge induced by the heating in the STCZ probably pushes the trough northward in experiment B and not in experiment D. Actually, the upper-level circulation in experiment D is similar to the results of a nonlinear modeling study for a tropical isolated heat source (Hendon 1986) in which no strong subtropical heat source is included. The low-level trough northwest of the STCZ observed in experiment B disappears in experiment D, and a strong subtropical high

[2] We can obtain almost the same composite fields in experiment B by referencing the development of a trough of the subtropical jet, instead of referencing the rainfall in the STCZ (not shown).

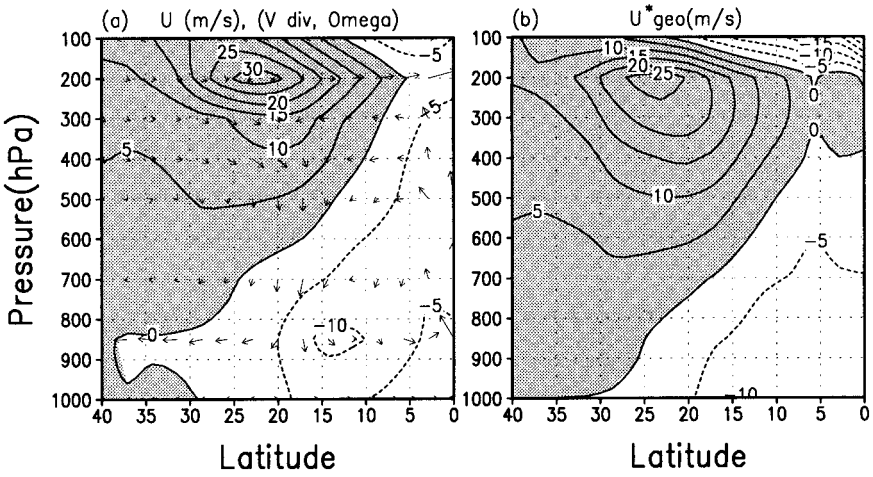

FIG. 16. As in Figs. 14c and 14d except for the active periods of experiment D.

covers the original position of the STCZ. Since the unnatural rainfall surrounding the dry region may intensify the subtropical high, we omit further discussion of the mechanisms of the high. However, we need to remark that the low-level trough accompanied by strong low-level southwest wind along the southeastern edge disappeared without the heating in the STCZ.

A drastic change is also observed in the composite cross section of wind along the line shown in Fig. 15a. A strong subtropical jet is significant only in the upper troposphere and does not extend downward and southward (Fig. 16a), which is different from the model STCZ in experiment B and the real STCZs in their active periods (cf. Figs. 14c and 10 of Kodama 1992). The geostrophic wind shown in Fig. 14b almost agrees with the composite wind (Fig. 14a), which means that the disappearance of the low-level wind along the STCZ is geostrophically related to the low-level trough disappearance.

As we remarked in section 3, westerlies of the subtropical jet along the model and real STCZs extend downward to the earth's surface when the STCZs are active, unlike the ordinary subtropical jets that appear only in the upper troposphere (e.g., Palmen and Newton 1969). Interestingly, the classic configuration of the subtropical jet agrees with the results in experiment D but not in experiment B in the active periods. The strong diabatic heating in the STCZ seems to intensify the low-level southwest wind connected to the upper subtropical jet and maintains the unique wind structure of the STCZ, unlike the ordinary subtropical jets.

Finally, we suggest that the STCZ radiates a stationary Rossby wave in the GCM. The upper panels of Fig. 17 show the composite fields of 500-hPa height and their anomalies from the zonal means for the active periods of the model STCZ in experiment B. The lower panels show corresponding composite fields in experiment D. In experiment B, a trough of the subtropical jet is developed at ~140°W around the STCZ, as discussed previously. A wave train from the trough toward the midlatitudes is significant in the anomaly height field (Fig. 17b). This train has a barotropic structure, that is, the height anomaly is almost in phase throughout the troposphere (not shown). In experiment D, on the other hand, no similar significant wave trains are found, in spite of our selecting the periods for the composite when a subtropical-jet trough was developed. The strong heating in the STCZ seems to be a significant vorticity source in the subtropics, where the mean westerlies are strong (Fig. 3). Therefore, it is natural that the real STCZs existed in the mean westerlies are sources of stationary Rossby waves, although no existing studies of this feature are known to the present author. In further observational studies, we need to investigate carefully whether the real STCZs radiate the Rossby waves.

8. Summary and discussions

Numerical experiments were done using an aqua-planet GCM to clarify the mechanisms that form the STCZ, especially the roles of the atmospheric diabatic heating in the tropical monsoons and in the STCZ. The main results can be summarized as follows.

1) An STCZ with several large-scale characteristics similar to the real STCZs appears in the aqua-planet GCM without any land when we put a monsoonlike, namely, strong zonally localized off-equatorial atmospheric heat source in the Tropics. This supports many previous findings on the close relationship between tropical monsoons and the real STCZs.
2) To maintain the STCZ, the monsoonlike heat source in the Tropics has two roles: one is to maintain a strong subtropical jet through an upper-level poleward divergent wind from the source. The other is to form a low-level poleward moisture flow toward the subtropics along the eastern periphery of a heat-induced depression around the heat source. Since this

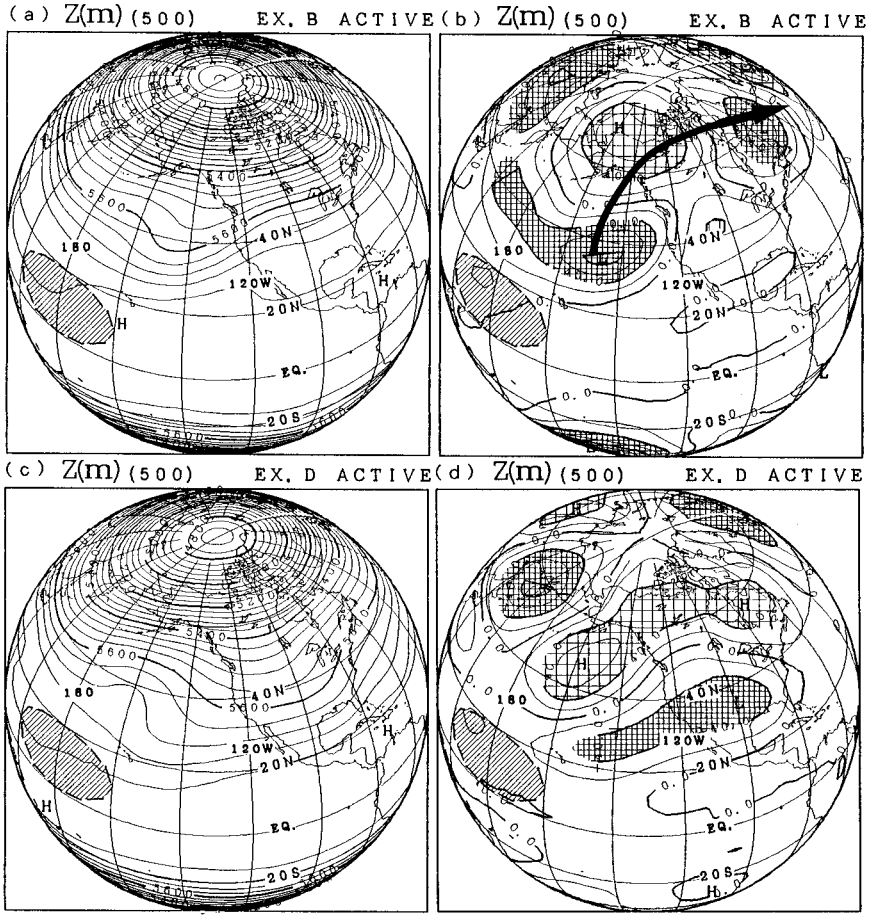

FIG. 17. Composite fields for the active periods of the model STCZ viewed from space in experiment B: (a) the 500-hPa height and (b) the 500-hPa height anomaly from the zonal mean. (c) and (d) are the same as in (a) and (b), respectively, except in experiment D. Contour intervals are 50 m in (a) and (c), and 20 m in (b) and (d). The hatched oval in each panel indicates the area of the warm water pool. The thick arrow in (b) indicates the path of a possible stationary wave train.

flow is driven by a pressure gradient that is intensified as the depression penetrates the subtropical-high belt, formation of the STCZ strongly depends on the latitude of the heat source.

3) Upward motion maintained by the strong heating in the STCZ is a significant vorticity source and sink in the lower and upper troposphere, respectively, and unique height fields form around the STCZs. In the lower troposphere, generation of positive vorticity by stretching is canceled by negative vorticity advection by a strong east and poleward wind along the STCZ. To maintain this wind, a low-level trough forms on the west and poleward side of the STCZ. In the upper troposphere, generation of negative vorticity by shrinking is compensated by positive vorticity advection by mean upper-level westerlies in a westward vorticity gradient around the STCZ. To maintain the gradient, a coupled trough and ridge appears on the west and poleward side and on the east and equatorward side of the STCZ, respectively. Figure 18 shows the atmospheric circulations induced by the diabatic heating in the STCZ schematically.
4) Since the low-level east and poleward wind along the STCZ is maintained by the heating in the STCZ, the westerly of the subtropical jet along the STCZ appears to extend downward to the surface unlike the ordinary subtropical jets in which westerlies disappeared in the lower troposphere. The low-level wind along the STCZ and the poleward flow induced by the tropical heat source meet along the STCZ and form the strong convergence necessary to maintain the active rainfall in the STCZ.
5) A stationary Rossby wave radiated by the diabatic heating in the model STCZ embedded in the mean westerlies is suggested, although it should be confirmed in the real atmosphere in further studies.

A close relationship between the development of the

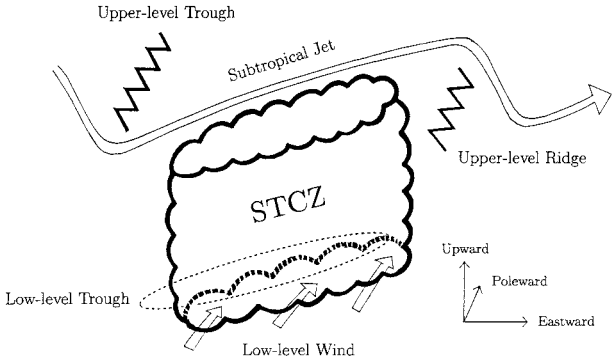

FIG. 18. A schematic view of the atmospheric circulations induced by the diabatic heating in the STCZ.

subtropical jet trough and rainfall activity of the real STCZ has been found observationally (Huang and Vincent 1983; Kiladis and Weickmann 1992) and in a modeling study (Kalnay et al. 1986). In our study, the trough is maintained by diabatic heating in the STCZ. On the other hand, Kiladis and Weickmann (1992) pointed out that the development of the trough preceded the intensification of rainfall in the SPCZ by one day. In our speculation, these two results are not in disagreement. The development of a trough seems to initiate strong rainfall because the trough shifts the jet accompanied by a potential front into lower latitudes with more moisture. After the rainfall starts, the trough is maintained by the heating in the STCZ, and the westerlies of the jet extend to the surface and maintain the strong moisture–flux convergence with the poleward moisture flow from the Tropics. The real STCZs frequently stagnate for up to 10 days (Vincent 1982; Kiladis and Weickmann 1992). The heating in the STCZs may contribute to the stagnation by maintaining the trough, although further studies on this speculation are necessary.

The east and poleward low-level wind along the STCZ may be identified with low-level jets, which are observed in the real STCZs along with severe convective storms (e.g., Ninomiya and Akiyama 1973). Diabatic heating by strong rainfall (e.g., Uccellini and Johnson 1979) and vertical momentum mixing by deep convection (e.g., Ninomiya 1971) have been reported to form the low-level jet. In our GCM, the vertical momentum mixing by deep convection is not included as in most of the other GCMs. Our results show that the heating can form the low-level wind along the STCZ. However, the contribution of the momentum mixing should be evaluated in the future by including this process in the GCM. The low-level wind along the STCZ, together with the poleward flow induced by the tropical heat source, maintains strong moisture convergence in the STCZ. Since the low-level wind along the STCZ is maintained by the diabatic heating in the STCZ, a positive feedback is expected between the rainfall activity and the wind along the STCZ, although a quantitative evaluation of the feedback is beyond this study.

The Tropical Rainfall Measuring Mission (TRMM) (Simpson et al. 1988) was launched in November 1997. We can expect to obtain 3D observations of the atmospheric diabatic heating from the TRMM observations. This information will be important and useful for studying the STCZs.

Acknowledgments. The author would like to express his special thanks to Dr. A. Numaguti of Hokkaido University for permitting me to use his aqua-planet GCM with his kind guidance. Thanks are extended to Prof. T. Asai and Prof. T. Nitta for their encouragement throughout this study. Discussions with Prof. M. Yamasaki, Dr. H. Nakamura, and Dr. S.-H. Xie were fruitful. Comments of anonymous reviewers were helpful in improving the original manuscript. We utilized NCEP–NCAR reanalysis data obtained from the NCAR data library compiled by Dr. H. Nakamura and Mr. A. Sinpo. This study was supported by the Grant-in-aid for Scientific Research by the Japanese Ministry of Education, Science, Sports, and Culture. Part of this study was done as a cooperative study with the University of Tokyo's Climate System Research and National Space Development Agency of Japan. The NCAR Graphics developed at NCAR and the Grid Analysis and Display System developed at COLA, University of Maryland, were utilized to draw the figures in this paper.

REFERENCES

Chen, T.-C., and J.-M. Chen, 1993: The intraseasonal oscillation of the lower-tropospheric circulation over the western Pacific during the 1979 northern summer. *J. Meteor. Soc. Japan,* **71,** 205–220.

——, M.-C. Yen, and M. Murakami, 1988: The water vapor transport associated with the 30–50-day oscillation over the Asian monsoon regions during 1979 summer. *Mon. Wea. Rev.,* **116,** 1983–2002.

Figueroa, S. N., P. Satyamurty, and P. L. Silva Dias, 1995: Simulations of the summer circulation over the South American region with the Eta coordinate model. *J. Atmos. Sci.,* **52,** 1573–1584.

Gandu, A. W., and J. E. Geisler, 1991: A primitive equations model study of the effect of topography on the summer circulation over tropical South America. *J. Atmos. Sci.,* **48,** 1822–1836.

Gill, A. E., 1980: Some simple solutions for heat-induced tropical circulation. *Quart. J. Roy. Meteor. Soc.,* **106,** 447–462.

Hendon, H. H., 1986: The time–mean flow and variability in a nonlinear model of the atmosphere with tropical diabatic forcing. *J. Atmos. Sci.,* **43,** 72–88.

Huang, H.-J., and D. G. Vincent, 1983: Major changes in circulation features over the South Pacific during FGGE, 10–27 January 1979. *Mon. Wea. Rev.,* **111,** 1611–1618.

Hurrell, J. W., and D. G. Vincent, 1990: Relationship between tropical heating and subtropical westerly maxima in the Southern Hemisphere during SOP-1, FGGE. *J. Climate,* **3,** 751–768.

——, and ——, 1991: On the maintenance of short-term wind maxima in the Southern Hemisphere during SOP-1, FGGE. *J. Climate,* **4,** 1009–1022.

Jaeger, L., 1976: Monthly precipitation for the whole world (in German). *Ber. Dtsch. Wetterdienstes,* **139,** 1–38.

Janowiak, J. E., P. H. Arkin, P. Xie, M. L. Morrissey, and D. R. Legates, 1995: An examination of the east Pacific ITCZ rainfall distribution. *J. Climate,* **8,** 2810–2823.

Kalnay, E., K. C. Mo, and J. Paegle, 1986: Large-amplitude, short-

scale stationary Rossby waves in the Southern Hemisphere: Observations and mechanistic experiment to determine their origin. *J. Atmos. Sci.,* **43,** 252–275.

Kato, K., 1989: Seasonal transition of the lower-level circulation systems around the Baiu Front in China in 1979 and its relation to the Northern Summer Monsoon. *J. Meteor. Soc. Japan,* **67,** 249–265.

Kiladis, G. N., and K. M. Weickmann, 1992: Extratropical forcing of tropical Pacific convection during northern winter. *Mon. Wea. Rev.,* **120,** 1924–1938.

——, H. von Storch, and H. van Loon, 1989: Origin of the South Pacific convergence zone. *J. Climate,* **2,** 1185–1195.

Kodama, Y.-M., 1992: Large-scale common features of subtropical precipitation zones (the Baiu frontal zone, the SPCZ, and the SACZ). Part I: Characteristics of subtropical frontal zones. *J. Meteor. Soc. Japan,* **70,** 813–836.

——, 1993: Large-scale common features of subtropical convergence zones (the Baiu frontal zone, the SPCZ, and the SACZ). Part II: Conditions of the circulations for generating the STCZs. *J. Meteor. Soc. Japan,* **71,** 581–610.

Kuo, H. L., 1974: Further studies of the parameterization of the influence of cumulus convection on large-scale flow. *J. Atmos. Sci.,* **31,** 1232–1240.

Lau, K.-M., and P. H. Chan, 1985: Aspects of the 40–50-day oscillation during the northern winter as inferred from outgoing longwave radiation. *Mon. Wea. Rev.,* **113,** 1889–1909.

Matsumoto, S., K. Ninomiya, and S. Yoshizumi, 1971: Characteristic features of Baiu front associated with heavy rainfall. *J. Meteor. Soc. Japan,* **49,** 267–281.

Murakami, M., 1984: Analysis of the deep convective activity over the western Pacific and Southeast Asia. Part II: Seasonal and intraseasonal variations during northern summer. *J. Meteor. Soc. Japan,* **62,** 88–108.

Murakami, T., L.-X. Chen, and A. Xie, 1986: Relationship among seasonal cycles, low-frequency oscillation, and transient disturbances as revealed from outgoing longwave radiation data. *Mon. Wea. Rev.,* **114,** 1456–1465.

Ninomiya, K., 1971: Mesoscale modification of synoptic situations from thunderstorm development as revealed by ATS III and aerological data. *J. Appl. Meteor.,* **10,** 1103–1121.

——, 1984: Characteristics of Baiu front as a predominant subtropical front in the summer Northern Hemisphere. *J. Meteor. Soc. Japan,* **62,** 880–894.

——, and T. Akiyama, 1973: Medium-scale echo clusters in the Baiu Front as revealed by multi-radar composite echo maps (Part II). *J. Meteor. Soc. Japan,* **51,** 108–118.

Numaguti, A., 1993: Dynamics and energy balance of the Hadley circulation and the tropical precipitation zones: Significance of the distribution of evaporation. *J. Atmos. Sci.,* **50,** 1874–1887.

Ose, T., 1998: Seasonal change of Asian summer monsoon circulation and its heat source. *J. Meteor. Soc. Japan,* **76,** 1045–1063.

Palmen, E., and C. W. Newton, 1969: *Atmospheric Circulation Systems: Their Structure and Physical Interpretation.* Academic Press, 603 pp.

Sardesmukh, P. D., and B. J. Hoskins, 1985: Vorticity balances in the Tropics during the 1982–83 El Niño–Southern Oscillation event. *Quart. J. Roy. Meteor., Soc.,* **111,** 261–278.

Simpson, J., R. F. Adler, and G. R. North, 1988: A proposed Tropical Rainfall Measuring Mission (TRMM) satellite. *Bull. Amer. Meteor. Soc.,* **69,** 278–295.

Ting, M., and I. M. Held, 1990: The stationary wave response to a tropical SST anomaly in an idealized GCM. *J. Atmos. Sci.,* **47,** 2546–2566.

Uccellini, L. W., and D. R. Johnson, 1979: The coupling of upper and lower tropospheric jet streaks and implications for the development of severe convective storms. *Mon. Wea. Rev.,* **107,** 682–703.

Vincent, D. G., 1982: Circulation features over the South Pacific during 10–18 January 1979. *Mon. Wea. Rev.,* **110,** 981–993.

Yamazaki, N., and T.-C. Chen, 1993: Analysis of the East Asian monsoon during early summer of 1979: Structure of the Baiu Front and its relationships to large-scale fields. *J. Meteor. Soc. Japan,* **71,** 339–355.